

5. S. K. Godunov, V. V. Denisenko, et al., "Use of a viscoelastic relaxation model in calculating uniaxial homogeneous strains and refining interpolation formulas for Maxwellian viscosity," Zh. Prikl. Mekh. Tekh. Fiz., No. 5 (1979).
6. A. G. Ivanov, "Spalling in the quasiaoustic approximation," Fiz. Goreniya Vzryva, No. 3 (1975).

CALCULATION AND EXPERIMENTS ON THE DEFORMATION OF
EXPLOSION-CHAMBER SHELLS

A. I. Abakumov, V. V. Egunov, A. G. Ivanov,
A. A. Uchaev, V. I. Tsytkin, and A. T. Shitov

UDC 620.178.7

It has been observed that there is a cyclic increase in the strain amplitude with the passage of time in experiments on the pulsed loading of explosion chambers [1, 2], which is due to interaction between some bending modes of the chamber called the critical with membrane forms of vibration, which results in an unstable state, with cyclic energy transfer from the membrane forms to the bending ones. The bending forms are excited by various structural components (tubes, supporting plates for instruments, welded joints, and so on), and also by imperfections represented by deviations in the geometrical and mechanical characteristics.

Here we compare theoretical results with experimental ones to show that the cyclic strain growth can be described by means of a shell theory of Timoshenko type incorporating the rotating inertia and the transverse shear.

1. Experimental Scheme and Results. We examined the deformation of a closed spherical shell made of steel 35 of internal radius 153 mm and thickness 13.5 mm filled with air under normal conditions when a charge was exploded within it.

Figure 1 shows the system and the main dimensions. The shell 1 was sealed by the rigidly fixed plug 2 and was suspended from the neck by a sheet of small acoustic rigidity and mass, which eliminated any effect from the supporting system on the dynamic strain. The spherical charge 5 made of TH 50/50 (50% trotyl and 50% hexagen, density 1.65 g/cm^3) was of mass $80 \pm 0.5 \text{ g}$ and was placed at the center of the shell and detonated from the center. The possible deviation of the charge center from the geometrical center of the shell was not more than 2 mm. The shell strain $\epsilon(t)$ was recorded at the equator and pole by strain gauges. In the equator region, the measurement was of the mean axially symmetrical strain performed by two ring wire sensors 3 [3]. In the region of the pole, we recorded the local strain over a base-line of 20 mm with two symmetrically disposed sensors 4. The centers of the sensors deviated from the pole by 10 mm. The recording was performed with S1-18 oscilloscopes. The maximum recording time was 2 msec. The maximum error in determining the strain was 10% and in the time intervals was 5%.

Table 1 gives the results of two identical experiments, where ϵ_1 and t_1 are correspondingly the strain at the first peak and the time when it was attained reckoned from the start of strain, while ϵ_{\max} and t_{\max} are the maximum strain and the time when it was attained. Figure 2, solid lines, shows the observed $\epsilon(t)$ at the equator and pole obtained by averaging the two experiments.

The results show as follows:

- 1) The average annular strain in the equatorial region and the local strain around the pole coincide during the first half-cycle; and 2) the maximum value of the mean annular strain in the equatorial region occurs during the first half-cycle (Fig. 2), while the maximum local strain at the pole is attained after several periods, i.e., one gets the transfer phenomenon recorded in [1].

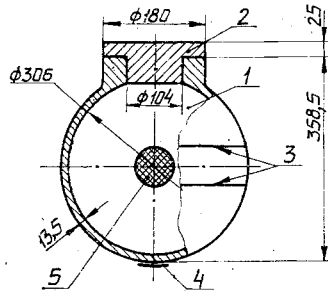


Fig. 1

TABLE 1

Experiment No.	$\epsilon_1, \%$		$t_1, \mu\text{sec}$		$\epsilon_{\text{max}}, \%$		$t_{\text{max}}, \mu\text{sec}$	
	equator	pole	equator	pole	equator	pole	equator	pole
1	0,09	0,08	55	52	0,09	0,23	55	560
2	0,08	0,08	50	50	0,08	0,22	50	540

2. Calculation Methods and Results. The state of strain was determined in two stages.

In the first stage, we determined the pressure profile $P = P(t)$ at the inner surface. $P(t)$ was determined by using a BESM-6 computer with a system of one-dimensional gasdynamic equations in spherical geometry with a boundary condition of rigid-wall type. The equation of state for the explosion products was taken in the form of [4], while the equation of state for air was taken from [5]. We used the difference method described in [6, 7] (exact Hugoniot analytic relations were used to calculate the states at the shock-wave front).

In the second stage, the theoretical $P = P(t)$ relation (Fig. 3) was used to describe the elastoplastic strain (Young's modulus of shell 210 GPa, dynamic yield point 0.5 GPa). The state of stress and strain was determined from the method of [8], which is based on equations from shell theory of Timoshenko type and physical relations from the differential theory of plasticity with linear kinematic hardening.

The equations of motion obtained from the principle of virtual displacements take the form

$$\frac{1}{r} \frac{\partial}{\partial s} [r(N_1 m + Qn)] + P_z = \rho h \ddot{z},$$

$$\frac{1}{r} \frac{\partial}{\partial s} [r(N_1 n - Qm)] - \frac{N_2}{r} + P_r = \rho h \ddot{r}, \quad \frac{1}{r} \frac{\partial}{\partial s} (rM_1) - \frac{M_2}{r} n - Q = \frac{\rho h^3}{12} \ddot{\varphi},$$

where N_i , M_i ($i = 1, 2$), Q are the forces, moments, and shearing force, h is thickness, ρ is shell material density, P_z and P_r are the projections of the intensity of the external load on the corresponding coordinate axes (z, r), φ is the angle of rotation of the cross section, and n and m are the direction cosines of the exterior normal to the surface.

We integrated the equations of motion with zero initial conditions by a finite-difference method using the explicit cross scheme. The time step was determined from the necessary condition for local stability $\Delta \tau \leq 0.95 \frac{\Delta s_{\text{min}}}{c}$. In view of the symmetry, we considered half of the

shell, with the median surface split up along the meridian into a series of nodes ($j = 0, 100$). In the method of [8], large deflections are incorporated by stepwise geometry adjustment.

The experimental strains may be compared with the calculated ones (dashed lines in Fig. 2) for the polar and equatorial regions; there is good agreement for the amplitude during the first period and also as regards the cyclic growth during the process. There are some differences due to the change in period in the experiment, which is due to using an idealized

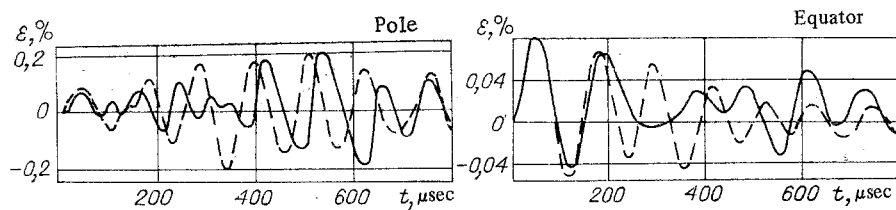


Fig. 2

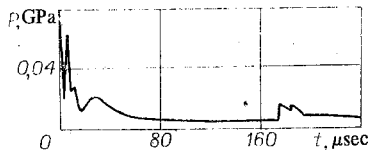


Fig. 3

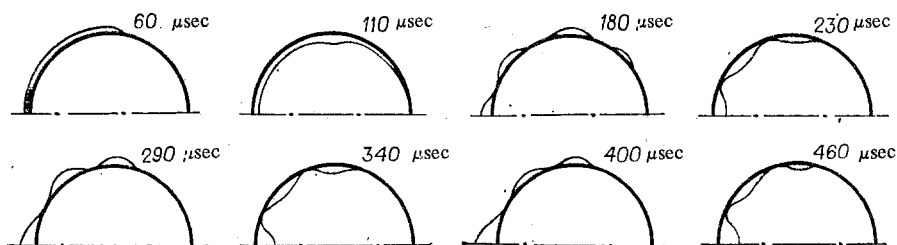


Fig. 4

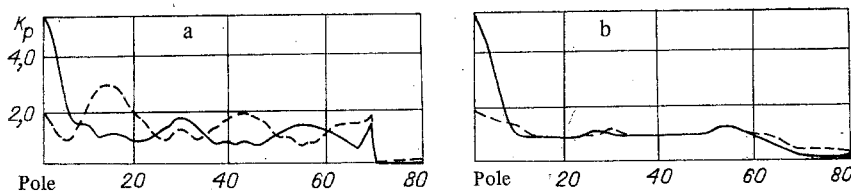


Fig. 5

theoretical scheme, which does not incorporate the actual imperfections, in particular the deviations from the nominal dimensions and mechanical characteristics. These imperfections and the adjoint mass lead to the bending-form spectrum being excited. The calculations show that for a sufficiently thick shell ($h/R > 1/20$) the adjoint mass has much more effect than the imperfections, which enables one to neglect the imperfections and to obtain results comparable with experiment.

Figure 4 shows the excitation of the bending forms at different instants after the start of deformation. It is evident that the bending forms in the meridian of the hemisphere propagate and increase in amplitude (the pole is on the left and the initial position is shown by the bold line).

The name shell pumping coefficient K_p is given to the ratio of the maximum strain at a particular point (in a particular computation cell) to the amplitude of the first period at the polar point. Figure 5 shows the distribution of K_p around the meridian on the outer surface (dashed curves) and the inner surface for meridional strains (a) and annular ones (b). Figure 5 shows that there are substantial differences in distribution of K_p at the outer and inner surfaces. The largest value is attained on the inner surface near the pole.

The agreement between the calculations and experiment for the most important characteristics indicates that the Timoshenko shell theory model describes the qualitative and quantitative aspects of the cyclic increase in strain amplitude quite accurately.

This cyclic amplitude increase occurs in local parts of the chamber, and the amplitude may become large, so the phenomenon must be incorporated in designing or developing explosion chambers.

LITERATURE CITED

1. A. A. Buzukov, "Behavior of explosion-chamber walls under pulsed loads," *Fiz. Goreniya Vzryva*, No. 4 (1976).
2. M. V. Kornev, V. V. Adishchev, et al., "An experimental study and analysis of the vibrations in the shell of an explosion chamber," *Fiz. Goreniya Vzryva*, No. 6 (1979).
3. A. T. Shitov, V. N. Mineev, et al., "A wire sensor for continuous recording of large strains in dynamic loading," *Fiz. Goreniya Vzryva*, No. 2 (1977).
4. V. N. Zubarev, G. S. Telegin, and M. V. Zhernokletov, "Expansion isentropes for the products from condensed explosives," *Zh. Prikl. Mekh. Tekh. Fiz.*, No. 4 (1969).
5. N. M. Kuznetsov, *Thermodynamic Functions and Shock Adiabatics for Air at High Temperatures* [in Russian], Mashinostroenie, Moscow (1965).
6. V. F. Kuropatenko, "A method of constructing difference schemes for the numerical integration of gasdynamic equations," *Izv. Vyssh. Uchebn. Zaved., Matematika*, No. 3(28) (1962).
7. V. F. Kuropatenko, "Difference schemes for the numerical integration of gasdynamic equations," *Trudy Mat. Inst. Akad. Nauk SSSR*, No. 74 (1966).
8. V. G. Bazhenov and V. K. Lomunov, "A study of elastoplastic buckling in shells of rotation under shock loading," in: *Applied Aspects of Strength and Plasticity*, Issue 2 [in Russian] (Vsesoyuz. Mezhvuz. Sb., Gor'k. Univ.) (1975).

COMPOUND-FAILURE POLAR-FAN DIAGRAMS

Yu. I. Fadeenko

UDC 539.375

The kinetic theory of failure gives a relationship between the lifespan τ and the applied stress σ as a formula typical of a thermally activated process:

$$\tau = \tau_0 \exp [(u - \gamma\sigma)/kT], \quad (1)$$

where τ_0 is the period of the relevant mode of thermal vibrations, and the exponential factor is a quantify reciprocal to the probability of an elementary act of failure (overcoming the activation barrier) in one period of oscillations, while u is activation energy, and γ is the activation volume.

Here we wish to point out that one can use the shape of the observed $\tau(\sigma)$ to judge how many elementary failure mechanisms make a substantial contribution to the lifespan. Here the polar-fan diagram technique is used.

It follows from (1) that the family of $\tau(\sigma)$ isotherms forms a fan of rectilinear rays in the $(\sigma, \ln \tau)$ plane emerging from the pole with coordinates $(u/\gamma, \ln \tau_0)$. If two different failure mechanisms are active together, there will be two different isotherm fans, and the resultant isotherms will have the form of kinked lines, as shown in Fig. 1. The experimental isotherms in fact sometimes have these kinks [1, 2]. In [1], it was assumed that the lifespan is determined always by a single universal failure mechanism, namely by the stage of initiation and growth of microscopically small cracks. The growth rates of these nuclear cracks increase rapidly with the lengths, and the total time for them to reach the critical Griffiths size is determined by the time required to reach a size of a few times the inter-atomic distance. Then τ_0 is of the order of the atomic vibration period, u is the energy of an elementary atomic bond intersected by the plane of the crack, and γ is the product of the effective stress concentration and the volume occupied by an atom. According to [1], the kink in $\tau(\sigma)$ corresponds to a stepwise change in the structure of the solid, and also in the structure-sensitive parameter γ (and evidently also in τ_0). The values of u should remain unchanged.

It may be that the concepts of [1] describe some particular cases of kinks on isotherms correctly, but in the general case one naturally assumes that the rectilinear parts of the kinked isotherms may be related to different physical mechanisms acting simultaneously. That